From Parkinsonian thalamic activity to restoring thalamic relay using deep brain stimulation: new insights from computational modeling

H G E Meijer[1], M Krupa[2], H Cagnan[3], M A J Lourens[1], T Heida[1], H C F Martens[3], L J Bour[4] and S A van Gils[1]

[1] Department of Electrical Engineering, Computer Science and Mathematics, University of Twente, PO Box 217, 7500 AE Enschede, The Netherlands
[2] Department of Medical Physics and Biophysics, University of Nijmegen, Geert Groteplein 21, 6525 EZ Nijmegen, The Netherlands
[3] Philips Research, High Tech Campus 34, 5656 AE Eindhoven, The Netherlands
[4] Department of Neurology/Clinical Neurophysiology, Academic Medical Center, University of Amsterdam, Meibergdreef 9, 1005 AZ Amsterdam, The Netherlands

E-mail: meijerhge@ewi.utwente.nl

Abstract

We present a computational model of a thalamocortical relay neuron for exploring basal ganglia thalamocortical loop behavior in relation to Parkinson's disease and deep brain stimulation (DBS). Previous microelectrode, single-unit recording studies demonstrated that oscillatory interaction within and between basal ganglia nuclei is very often accompanied by synchronization at Parkinsonian rest tremor frequencies (3–10 Hz). These oscillations have a profound influence on thalamic projections and impair the thalamic relaying of cortical input by generating rebound action potentials. Our model describes convergent inhibitory input received from basal ganglia by the thalamocortical cells based on characteristics of normal activity, and/or low-frequency oscillations (activity associated with Parkinson's disease). In addition to simulated input, we also used microelectrode recordings as inputs for the model. In the resting state, and without additional sensorimotor input, pathological rebound activity is generated for even mild Parkinsonian input. We have found a specific stimulation window of amplitudes and frequencies for periodic input, which corresponds to high-frequency DBS, and which also suppresses rebound activity for mild and even more prominent Parkinsonian input. When low-frequency pathological rebound activity disables the thalamocortical cell's ability to relay excitatory cortical input, a stimulation signal with parameter settings corresponding to our stimulation window can restore the thalamocortical cell's relay functionality.

1. Introduction

Parkinson's disease (PD) is a neurodegenerative disorder characterized by the loss of nigrostriatal dopaminergic neurons and accompanied by abnormal synchronous oscillatory activity at multiple levels of the basal ganglia–cortical loop (Hammond *et al* 2007). The primary motor symptoms of the disease are tremor at rest, bradykinesia, akinesia and rigidity. Deep brain stimulation (DBS) is a established technique to alleviate these symptoms. DBS can be applied in several nuclei including the subthalamic nucleus (STN) (Hashimoto *et al* 2003, Levy *et al* 2000), globus pallidus interna (GPi) (Anderson *et al* 2003) and the ventral intermediate thalamic (VIM) nucleus (Benabid 2003). Thalamic DBS is

mainly effective in reducing tremor; however, when DBS is predominantly applied at the STN or GPi, it relieves other PD motor symptoms, including rigidity and bradykinesia. A prospective study of 49 patients who were treated with bilateral STN stimulation resulted in an average improvement of their UPDRS scores at 5 years for motor functions by 54% ($p < 0.001$), while off medication, and those for activities of daily living improved by 49% ($p < 0.001$), as compared with base line (Krack *et al* 2003). Remarkably, DBS was only effective for the different target nuclei within very specific parameter ranges, most notably at high frequencies (>100 Hz) and with lower amplitudes at higher frequencies (Rizzone *et al* 2001, Moro *et al* 2002). These parameter settings for DBS are based on several studies (Benabid *et al* 1991, Limousin *et al* 1995, Volkmann *et al* 2002, 2006). Despite high clinical success rates, the mechanism by which DBS prevents pathophysiological responses of the motor network remains unknown. Several hypotheses regarding DBS's effectiveness have been formulated, including (1) stimulation-induced disruption or desynchronization of pathological network activity (McIntyre *et al* 2004, Tass 2001, Benabid *et al* 2009, McIntyre and Hahn 2010), (2) downstream effects of axonal activation such as synaptic inhibition or regularization of GPi activity (McIntyre *et al* 2004, Rubin and Terman 2004, Benabid *et al* 2009, Johnson *et al* 2008, Montgomery and Gale 2008), (3) resonances in the cortico-basal ganglia–thalamocortical loop (Montgomery and Gale 2008) and (4) anti-dromic stimulation of afferent axons projecting to the stimulated nucleus (Gradinaru *et al* 2009). In this study, we focus on a combination of downstream effects and regularization of activity.

The pathophysiology of PD is characterized by increased firing rates of neurons in the basal ganglia (BG), and a tendency toward bursting and abnormal synchronization in the neurons of STN and globus pallidus (GP) (Brown 2003). Experimental studies have linked synchronization that occurs at frequencies within the 3–10 Hz-band and beta band (15–30 Hz) with PD. The beta (15–30 Hz) oscillations are probably driven from the motor areas of the cortex, but at tremor frequencies (i.e. 3–10 Hz) it is the opposite direction of connectivity that dominates the synchronized activity. Coherence between STN and GPi activity has been confirmed at tremor frequencies; moreover, STN activity leads to activity in the GPi (Brown *et al* 2001). Additionally, these nuclei showed coherence between the GPi's thalamic projection site, the ventralis anterior thalami and the cortex. This coherence is also characterized by thalamic activity preceding cortical activity (Brown 2003). These findings emphasize the influence of the oscillatory mode in the STN and GPi on the cortico-basal ganglia-thalamocortical circuit at tremor frequencies. In this circuit, the thalamus is in a key position as it receives the convergent afferent input from the GPi, the cortex and the peripheral system, which it then projects back to the cortex, including motor areas (Smith *et al* 1998).

When thalamic neurons become hyperpolarized for 50–100 ms at tremor frequency, they show oscillatory bursting patterns (Jahnsen and Llinàs 1984). The ionic mechanism underlying this rebound behavior is the slow, low-threshold T-type Ca^{2+} current. Responses of thalamic neurons to afferent (inhibitory) signals from the GPi under both PD and DBS conditions would appear to be vital to our understanding of the DBS mechanism(s). This conclusion is also supported by findings showing that DBS modulates the BG's output, as received by thalamus, rather than restores it to a normal state (Dostrovsky and Lozano 2002, Hashimoto *et al* 2003, Rubin and Terman 2004). In their pioneering work, Rubin and Terman (2004) strongly indicated that the thalamic relay function could be restored by STN-DBS-induced synchronized activity at high frequencies (i.e. around 167 Hz, somewhat higher than the commonly clinically used frequency of 130–145 Hz). They also showed that the input from the BG with Parkinson-related frequency content (<30 Hz) impaired thalamic processing. Their later computational model used a single thalamocortical (TC) relay cell, as well as a heterogeneous population of TC cells, to determine TC relay fidelity. This model used both simulated BG output and experimentally recorded GPi spike trains from normal (control) monkeys and from Parkinsonian (MPTP) monkeys (Guo *et al* 2008). Similar conclusions could be reached based on inputs for the TC neuron model from both the simulated and recorded GPi activity. The results of these computational studies have led to significant advances in understanding the mechanism underpinning the efficacy of (STN-)DBS. However, results validating the existence of a clinically effective stimulation window that combines low-stimulation amplitudes and high frequencies have yet to be presented.

The aim of this study, which complements the work of Rubin and Terman, is to explore the amplitude and frequency dependence with respect to the generation and suppression of rebound activity in a TC relay cell. We modeled a single TC relay neuron and simulated input conditions that represent the characteristic behavior of the BG network. Therefore, irrespective of the exact network architecture, BG output is considered as an integrated signal representing normal, Parkinsonian and stimulation-induced activity patterns conforming to experimental data. This takes into account the fact that a group of GPi neurons converges onto a single, thalamic cell (Raz *et al* 2000, Smith *et al* 1998). The model was also simulated using microelectrode recordings (MER) from the GPi as input for the model. The power spectrum of this input has a prominent peak around 5 Hz. As a result, we focus primarily on the effectiveness of the stimulation with respect to PD tremor reduction.

2. Methods

We investigated the response of a TC neuron for a frequency range of 0–200 Hz corresponding to normal constant input resulting from the integration of irregular firing patterns, low-frequency signals (3–30 Hz; associated with Parkinsonian oscillatory behavior and/or low-frequency electrical stimulation), and for signals representing high-frequency stimulation (>30 Hz). The input based on recorded GPi data is combined with an idealized signal representing electrical stimulation for a frequency range from 0 to 200 Hz.

In addition, a simplified model signal for the Parkinsonian input is considered to study the frequency dependence and the role of synchronization in the generation of rebound responses.

We also took a number of conditions into consideration as follows. First, the output from GPi is synaptically transmitted to the TC relay cell. Secondly, pathological oscillations due to PD are assumed to remain (partially) present in BG output when stimulation is applied. This is in accordance with clinical observations showing that firing patterns of some STN neurons appear unaltered during DBS at standard settings (Carlson *et al* 2010) and that PD symptoms prevail during sub-therapeutic DBS (Moro *et al* 2002, Rizzone *et al* 2001, Hashimoto *et al* 2003, Butson and McIntyre 2005). Stimulation might only affect part of the stimulated nucleus and corresponding pathways in the BG (Johnson and McIntyre 2008). We therefore also assume that the GPi output is due to both the stimulation and remaining pathological Parkinsonian activity in the BG. The presence of oscillatory, low frequency inputs from the GPi (3–10 Hz) assumes a central oscillator within the BG, which would also be responsible for Parkinsonian rest tremor (Deuschl *et al* 2000). Thirdly, we are aware that DBS may act through electrical high-frequency stimulation of either STN or GPi, via orthodromic and/or antidromic activation of efferent and/or afferent axons. Irrespective of the target nucleus, we assume that the DBS-induced, high-frequency patterns are transmitted through the BG network and result in a tonic high-frequency synaptic input to the thalamus through GPi (Lozano *et al* 2002). Regarding STN-DBS, in an earlier computational model of a small BG network we showed that the DBS frequency is transmitted via the GPi output to the thalamus (Cagnan *et al* 2009). Fourthly, the response to pathological synchronized oscillatory input from the BG is considered with and without additional excitatory (sensorimotor) inputs. In the absence of external excitatory inputs, we assume that the thalamic relay cell should not spike. This represents a physiological resting state.

2.1. The TC relay neuron model

The TC relay neuron is represented by a single compartment model with membrane dynamics based on earlier modeling work (McIntyre *et al* 2004, Cagnan *et al* 2009) and neurophysiological data (Huguenard and McCormick 1992, McCormick and Huguenard 1992, Destexhe *et al* 1998). All currents are conductance based except for the T-type calcium current, which includes the Goldman–Hodgkin–Katz ion current equation. It can be concluded from experimental studies that highest T-current densities are found in distal dendrites (dendritic region at >11 μm from the soma). Without including dendritic compartments T-type channel behavior can be included in the single compartment model under the constraint that its I–V curves are similar to those of intact cells (Destexhe *et al* 1998). In this way, the model enables the generation of low-threshold burst responses consistent with experiments. The time derivative of the

membrane potential V of the thalamic neuron, the gating variables and the calcium concentration are given by

$$\begin{cases} C\dfrac{\mathrm{d}V}{\mathrm{d}t} = -(I_{\mathrm{Na},t} + I_{\mathrm{K},DR} + I_{\mathrm{K},s} + I_T + I_h + I_A \\ \qquad\quad + I_{\mathrm{Na,leak}} + I_{\mathrm{K,leak}} + I_{\mathrm{GPi,Th}} + I_{\mathrm{Ctx,Th}}), \\ \dfrac{\mathrm{d}X}{\mathrm{d}t} = (X_\infty - X)/\tau_X, \\ \dfrac{\mathrm{d}[\mathrm{Ca}]_i}{\mathrm{d}t} = ([\mathrm{Ca}]_{\mathrm{buf}} - [\mathrm{Ca}]_i)/\tau_{\mathrm{Ca}} - k_{\mathrm{Ca}} I_T. \end{cases} \quad (1)$$

Here, $I_{\mathrm{Na,leak}}$ and $I_{\mathrm{K,leak}}$ represent sodium and potassium leak currents, respectively, $I_{\mathrm{K},DR}$ represent fast, $I_{\mathrm{K},s}$ slow and I_A inactivating potassium currents, $I_{\mathrm{Na},t}$ is a transient sodium current, I_T is a low-threshold T-type Ca^{2+} current and I_h stands for a hyperpolarization-activated current. The synaptic input received by the thalamic cell from GPi neurons is described as $I_{\mathrm{GPi,Th}}$. Excitatory input from the cortex is described by $I_{\mathrm{Ctx,Th}}$. The gating variables $X \in \{m, k, n, m_T, h_T, c, d, e_{1,2}, f_{1,2}, h_{1,2}\}$ satisfy first-order differential equations. The functions X_∞ and τ_X are described in the appendix, but we briefly mention here that currents are expressed in μA cm^{-2}, conductances in mS cm^{-2}, times are in ms, voltages in mV and concentrations in mM).

In the absence of inputs from the GPi or the cortex, the TC cell is understood to be at rest at a potential near -60 mV. The application of a depolarizing input current results in a tonic spiking mode, whereas the TC cell's response to a release from a hyperpolarizing input current elicits a train of action potentials, i.e. a rebound burst (Smith *et al* 2000, Sherman 2001, Destexhe and Sejnowski 2003). Both simulated responses are shown in figure 1. T-type calcium channels play an important role in the generation of the post-inhibitory rebound action potentials. In particular, the T-inactivation variable h_T de-inactivates when the neuron receives inhibitory (synaptic) input. Upon release from inhibition, the membrane potential repolarizes to the rest membrane potential. The T-activation gate m_T acts on a much shorter time scale than h_T, and this results in the T-type Ca^{2+} channels remaining open for a limited amount of time. This calcium current depolarizes the neuron and rebound spikes are observed until h_T is again inactivated, thereby decreasing the T-type current. The A-current restrains the effect of T-type current (Pape *et al* 1994, Molineux *et al* 2005). Initially, we set $g_A = 0$ and next we investigate the influence of the inactivating potassium current I_A on our results.

2.2. Inputs to the TC neuron model

2.2.1. Characteristics of GPi Parkinsonian activity derived from MER data.
GPi single unit activity was retrieved from a single patient with advanced PD who received a DBS electrode implantation in the GPi. The procedure for DBS was a one-stage bilateral stereotactic approach, using frame-based three-dimensional MRI reconstructions for target calculations and path-planning, including MER. The standard target coordinates used were 21 mm lateral to the midplane, 2 mm anterior to the midcommissural point and 5 mm below the intercommissural point for the GPi. The patient was awake during the surgical procedure and
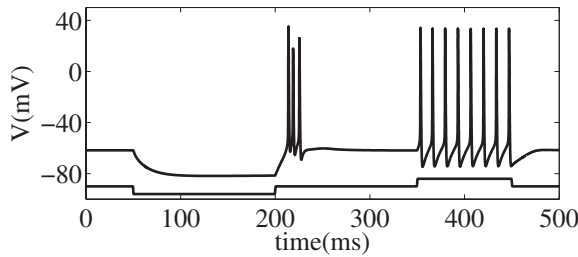
Figure 1. Response of the TC neuron model to input currents. Upon release of a hyperpolarizing input current (2 μA cm^{-2} applied for 150 ms starting at $t = 50$ ms), a rebound burst appears, while the neuron fires tonically in response to a depolarizing input (2 μA cm^{-2} for 100 ms starting at $t = 350$ ms and $g_A = 0$).

without any sedatives. Surgery and MER were performed following overnight withdrawal of anti-Parkinson medication. Extracellular single/multi-unit MER was performed with small (10 μm width) polyamide-coated tungsten microelectrodes (Medtronic; microelectrode 291; impedance 1.1 ± 0.4 MΩ; measured at 220 Hz, at the beginning of each trajectory) mounted on a sliding cannula. Signals were recorded with the amplifiers (10 000 times amplification) of the Leadpoint system (Medtronic), and were analog bandpass filtered between 500 and 5000 Hz (-3 dB; 12 dB/oct). The signal was sampled at 12 kHz, by use of a 16 bit A/D converter and afterward up-sampled to 24 kHz offline. Following a 2 s signal stabilization period after electrode movement cessation, multi-unit segments were recorded for 5–40 s. Starting for GPi 12 mm above the MRI-based target, the microelectrodes were advanced in steps of 500 μm toward the target by a manually controlled microdrive. When the needles were inside the GPe (globus pallidus externus) and GPi at each depth the spiking activity of the neurons lying close to the needle (an area with a radius up to about 200 μm) could be recorded. Depending on the neuronal density, no more than 3–5 units were recorded simultaneously. More distant units were indistinguishable from the background level. More details can be found in Bour *et al* (2010). Spikes were identified using the envelope method (Dolan *et al* 2009). On the basis of spike sorting we selected only those spikes that were most likely due to a single cell. The first 5 s of the spike train are shown in figure 2(A), and see figure 4(A) for a detailed enlargement. The power spectrum of the signal was then calculated according to Halliday *et al* (1995) and showed a strong frequency component near 5 Hz in the theta band, coherent with the Parkinsonian tremor of the patient's arm (Bour *et al* 2010), see figure 2(B).

2.2.2. Normal and Parkinsonian GPi output patterns.

The input $I_{\text{GPi,Th}}$ is assumed to be a convergent (GABA-ergic) inhibitory input from GPi (Smith *et al* 1998). This input may contain constant background activity representing normal (physiological) activity, oscillatory Parkinsonian activity and DBS-induced activity. It is described as

$$I_{\text{GPi,Th}} = (g_{\text{PD}}s_{\text{PD}}(t) + g_{\text{DBS}}s_{\text{DBS}}(t))(V - E_{\text{GABA}}). \quad (2)$$

The synaptic variable $s_{\text{PD}}(t)$ is modeled as an impulse response that decays exponentially with time constant $\tau_{\text{GABA}} = 10$ ms (i.e. $s(t) = \exp(-(t - t_i)/\tau_{\text{GABA}})$ with t_i the
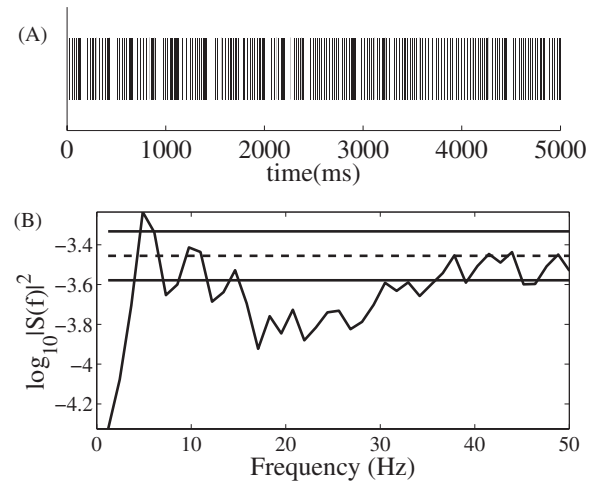

Figure 2. (A) First 5 s of the experimental GPi spike train. Each bar represents a spike. (B) Autospectrum of the experimental GPi time series with $S(f)$ the Fourier transform of the spike times. Asymptotic value of the spectrum (dashed) and 95% confidence levels (solid) are also indicated. There is a significant peak near 5 Hz.

time of the most recent GPi action potential). The GPi spike times for Parkinsonian conditions were taken from the experimentally recorded GPi time series as described above. A characteristic time series of the input is shown in figure 4(B), in which a typical tremor frequency of 5 Hz can be observed. The DBS signal (second term of (2)) has a periodic, exponentially decaying pulse shape $s_{\text{DBS}}(t) = \exp(-\text{mod}(t, 1000/f_{\text{DBS}})/\tau_{\text{GABA}})$ with f_{DBS} the stimulation frequency. This represents highly synchronized activity being transmitted to the thalamus via the GABAergic projection from the GPi regardless of whether the nucleus targeted by DBS is the STN or GPi. The parameters g_{PD} and g_{DBS} represent the maximum conductances of the signals. During DBS, the activity of the target nucleus is partially overwritten, depending on the volume of tissue activated (McIntyre *et al* 2004, Butson and McIntyre 2005, Hahn and McIntyre 2010). Indeed, some studies show a minor improvement of symptoms for subtherapeutic stimulation amplitudes (Hashimoto *et al* 2003, Guo *et al* 2008). This motivated us to use $g_{\text{PD}} = g_{\text{PD,max}}(1-\lambda)$ and $g_{\text{DBS}} = \beta g_{\text{PD,max}}\lambda$. We varied $g_{\text{PD,max}}$ to gauge how strong the GPi output should be in order to elicit pathological oscillatory responses in the thalamic neuron model. The recruitment factor λ between 0 and 1 represents the fraction of the input that is now due to DBS. The parameter β accounts for an increase in activity within the target nucleus due to electrical stimulation. For previously quiescent cells that may become active upon stimulation, the range is from 1 to 2 (Reese *et al* 2008, Hahn *et al* 2008). Finally, we set $E_{\text{GABA}} = -85$ mV for the GABA reversal potential (Rubin and Terman 2004, McIntyre *et al* 2004).

In order to perform a thorough analysis of the thalamic neuron model, a complete range of the frequencies associated with low-frequency Parkinsonian oscillatory activity is required. And since the single-unit activity data retrieved from MER only contain a 5 Hz tremor component, we needed an additional representation of GPi input. We therefore used

a waveform consisting of a dc component and the dominant frequency of oscillation:

$$I_{\text{GPi,Th}} = g_{\text{GPi,Th}}(1 + \alpha_P \sin(2\pi f_P t))(V - E_{\text{GABA}}). \quad (3)$$

This waveform is characterized by an average activity level $g_{\text{GPi,Th}}$ and oscillation frequency f_P. The parameter α_P is a modulation amplitude that gives a measure of the synchronization level within GPi; its value ranges between 0, or no Parkinsonian input, and 1, or complete synchronization. For equation (3) we have $g_{\text{PD,max}} = g_{\text{GPi,Th}}(1 + \alpha_P)$.

2.2.3. Sensorimotor input.

The excitatory (glutamatergic) synaptic input from the cortex, $I_{\text{Ctx,Th}}$, is modeled as a sequence of block pulses $s_{\text{Ctx,Th}}(t)$ with a pulse width of 5 ms ($s = 1$ during the pulse and $s = 0$ otherwise) and pulse amplitude g_{exc}. This is similar to Rubin and Terman (2004) and Guo *et al* (2008):

$$I_{\text{Ctx,Th}} = g_{\text{exc}} \, s_{\text{Ctx,Th}}(t) \, (V - E_{\text{Glut}}). \quad (4)$$

The reversal potential for glutamate (AMPA receptors) is $E_{\text{Glut}} = 0$ mV (Kim *et al* 1997, Destexhe *et al* 1998, Terman *et al* 2002, Rubin and Terman 2004, McIntyre *et al* 2004).

2.3. Simulation protocol

Time signals were computed with the aid of MATLAB (version 7.3, The MathWorks, Inc.) and by using 'ode15s' with maximal timestep 0.1 ms for solving the differential equations. Input patterns are defined to enable investigation of switches from normal to Parkinsonian behavior; the effect of high-frequency stimulation on oscillatory behavior and the TC cell's ability to perform its relaying function of sensorimotor input signals. The numerical bifurcation analysis of the TC model was performed using the MATLAB toolbox MATCONT, a continuation and bifurcation toolbox for the interactive numerical study of dynamical systems (Dhooge *et al* 2003). Periodic orbits have been computed using 80 mesh points and standard tolerances.

2.3.1. Normal and PD patterns.

We distinguish between normal and PD responses based on the appearance of rebound responses. The response of the TC cell was investigated with GPi input only (i.e. without high-frequency stimulation and sensorimotor input ($g_{\text{DBS,max}} = g_{\text{Ctx,Th}} = 0$ mS cm^{-2})). First, we increased $g_{\text{PD,max}}$ to a value where the low frequency oscillations in the experimental GPi time series elicited rebound responses. Subsequently, we considered the sensitivity of our results with respect to the level of synchrony and frequency using (3). To that end, we varied the parameters of the synaptic input $g_{\text{GPi,Th}}$, f_P and α_P. Initially, f_P in (3) is set to 8 Hz and $g_{\text{Gpi,Th}} = 0.1$ mS cm^{-2}. When we increase α_P, there is a critical value α_{c1}, which indicates the threshold between the generation of subthreshold oscillations and rebound spikes. We then reversed the direction, starting at $\alpha_P = 1$ and decreasing α_P, to discover α_{c2} implying a threshold between the generation of rebound spikes and subthreshold oscillations. Both thresholds α_{c1} and α_{c2} are detected automatically within MATCONT. We determined both critical values while varying $g_{\text{Gpi,Th}}$ and $f_P < 20$ Hz.

2.3.2. Stimulation induced patterns—rebound suppression and relay reliability.

By applying a stimulation signal we investigated if, how and under which conditions application of high-frequency inhibitory input to thalamus would prevent the TC cell from responding to a synchronized pathological drive (<30 Hz). Here, we used only the experimentally recorded GPi time series for the Parkinsonian signal.

To analyze the performance of stimulation in suppressing rebound responses we defined the suppression level S as the ratio of the number of suppressed rebound spikes and the number of rebound spikes without stimulation. When a rebound response consisted of multiple spikes, it was counted as one response. We tested the relay function of the TC cell using the relay level R in the presence of cortical excitatory input pulses, and with R defined as the ratio of successfully relayed input pulses and the number of excitatory pulses. The expected relay spike times are based on the excitatory input and aid in classifying the generating mechanism for each of the TC cell's action potentials. We make a distinction between responses to excitatory input pulses and rebound responses to synchronized inhibitory burst input from GPi. The definition of the suppression and relay level enables the separate investigation of the two different responses that may be attributed to pathology: the inability of relaying sensorimotor signals, and the generation of rebound responses resulting in transmission of BG oscillatory content to cortex ($S > 0.9$ is considered to indicate sufficient rebound suppression and $R > 0.9$ to indicate sufficient relay).

Simulations were performed for stimulation frequencies starting at 20 Hz up to 200 Hz (specifically 20, 25, 30 to 100 in steps of 10, 135, 185 and 200 Hz). We varied λ, the level of overwriting PD activity, between 0 and 1 (with an average step size of 0.05). We used $g_{\text{PD,max}} = 0.4$ mS cm^{-2} and tested $\beta = 1.0, 1.2, 1.5, 2.0$. For the excitatory input level we used $g_{\text{exc}} = 0.13, 0.15$ or 0.17 mS cm^{-2}. Lower values lead to a low success rate, while for values larger than 0.2, each excitatory input yields two TC spikes which we also classify as a bad relay. The timing of the excitatory pulses is stochastic. We take the interpulse interval from an exponential distribution with a mean of 60.6 ms (a rate of 16.5 Hz). We then imposed a minimal interpulse interval of 10 ms similar to Rubin and Terman (2004), Guo *et al* (2008) to prevent overlapping which would make classification ambiguous. We generated five such input trains, determined the maximal and minimal λ for sufficient relay and suppression, respectively, for each train and averaged over these five values. Additionally, in order to test the sensitivity of the model neuron, we increased the maximum permeability level of calcium, p_{Ca}, corresponding to the strength of the T-type Ca^{2+} current, from 0.1 to 0.15 10^{-3}cm s^{-1}. We also compared the R and S curves when the A-current was included in the model. The simulation of each of the conditions spans a period of 40 s.

3. Results

3.1. Normal and PD modes of the TC cell

We simulated the TC response with input according to (2) while increasing $g_{\text{PD,max}}$ from 0 to 0.5 mS cm^{-2} without DBS
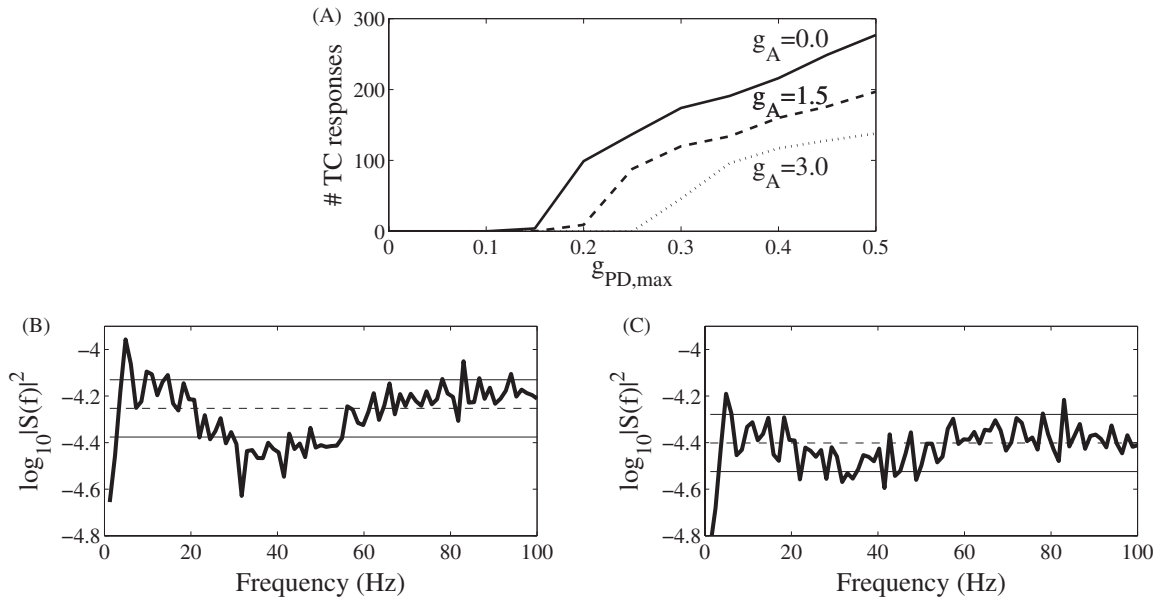
Figure 3. Characteristics of the response of the TC cell to GPi input. (A) The number of rebound responses as a function of $g_{PD,max}$. For $g_{PD,max} > 0.35$ some rebound responses consist of multiple spikes. For increasing values of g_A the number of responses diminishes (dashed and dotted lines). Power spectrum of the TC response for $g_{PD,max} = 0.5 \text{ mS cm}^{-2}$ and $g_A = 0 \text{ mS cm}^{-2}$ (B) and $g_A = 1.5 \text{ mS cm}^{-2}$ (C) with $S(f)$ the Fourier transform of the TC spike times. The dashed horizontal lines indicate the asymptotic values. The solid horizontal lines demarcate the 95% confidence intervals with two peaks above, one near 5 and the other around 90 Hz. The first is due to the GPi burst frequency, and the second due to bursts consisting of multiple spikes. The spectra without and with the A-current are very similar apart from a scaling factor as with the A-current there is less power.

input ($g_{DBS} = g_{exc} = 0$). For small $g_{PD,max}$ there is only subthreshold TC activity, while the TC cell shows rebound activity above a threshold of $g_{PD,max} \approx 0.15 \text{ mS cm}^{-2}$, see figure 3(A) (solid line). During 40 s of the simulation the TC cell has around 200 spikes for sufficiently high $g_{PD,max}$ which results in a frequency around 5 Hz. This is confirmed in the power spectrum, see figure 3(B). We concluded that the TC cell is transmitting the low frequency GPi oscillation. It is known that the A-current influences the generation of calcium T-type rebound responses (Pape *et al* 1994, Molineux *et al* 2005). For subthreshold values of the potential, these currents have an opposite effect. While the T-current is depolarizing, the A-current is hyperpolarizing, which makes it more difficult to spike. We have investigated this interplay for various values of the conductance g_A. First, for increasing values of g_A the minimal value of $g_{PD,max}$ that generates rebound responses increases. For very high values of g_A no rebound responses appear at all. Second, we see that fewer rebound responses are generated for increasing g_A. This can be understood by inspecting the time series as follows.

The rebound responses of the TC cell occur during silent intervals after a GPi burst (see figure 4(A–D)). During the GPi burst, the T-current de-inactivates providing the depolarizing drive for the post-inhibitory spike. Note that also a longer pause can lead to a response, e.g. around $t = 2750$ ms. When we include the A-current, e.g. we set $g_A = 1.5 \text{ mS cm}^{-2}$, we observe that the rebound response around $t = 2750$ ms disappears. The GPi input pause is not preceded by a true burst so that the T-current is only moderately strong. At this moment the A-current provides enough hyperpolarizing

current to counteract the drive by the T-current. We concluded that the A-current acts as a filter such that only GPi bursts cause rebound responses.

Next, we investigated variations of the model and the synaptic input using equation (3). Initially f_P in equation (3) is set to 8 Hz and $g_{GPi,Th} = 0.1 \text{ mS cm}^{-2}$. When simulating the input into the TC cell according to (3) and while no synchronization is present within GPi, i.e. $\alpha_P = 0$, the input is constant and the neuron responds by settling to a steady state. For small α_P the membrane potential responds with small sub-threshold oscillations. When increasing α_P from 0 to 1 it is observed that for values of α_P below a critical value, α_{c1}, no rebound action potentials are generated. Above this value, however, the thalamic neuron will always fire (at least once per period). When the experiment is reversed by decreasing α_P from 1 to 0 until the rebound action potential disappears, the critical value α_{c2} then becomes smaller than α_{c1}, indicating a region of bistability. Figure 5 shows both critical values as a function of the frequency of the Parkinsonian oscillations. From this figure we conclude that the frequency selectivity of the thalamic neuron model has a large overlap with experimentally observed frequencies related to synchronized activity during PD (Brown *et al* 2001, Magill *et al* 2000, Magnin *et al* 2000, Nini *et al* 1995, Raz *et al* 2000). This is specifically true for higher values of α_P, which indicates that input from GPi is more synchronized, and synaptic input with frequencies in a Parkinsonian regime can elicit rebound action potentials continuously. For a frequency f_P of 8 Hz, at which value the threshold level is near a minimum, $\alpha_{c1} = 0.81$ and $\alpha_{c2} = 0.79$.
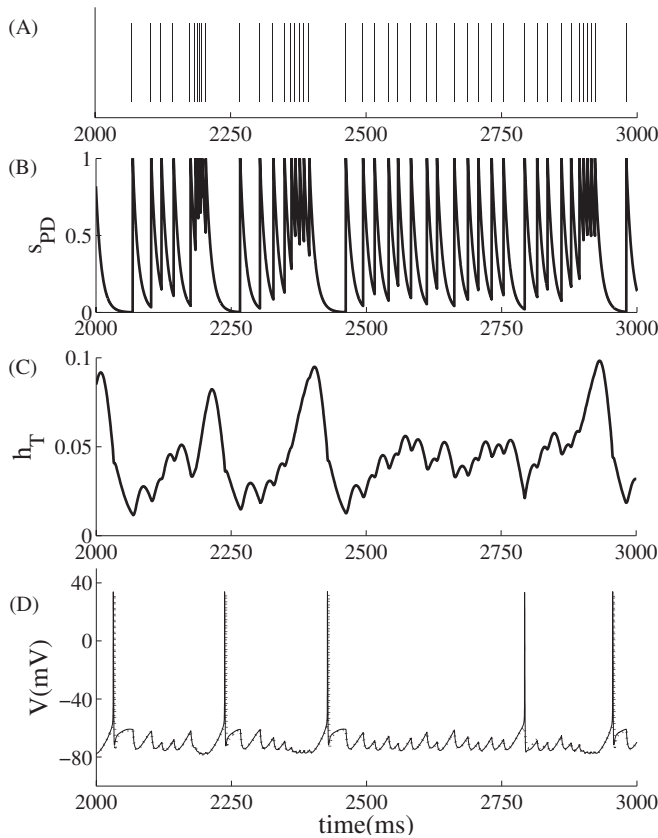
Figure 4. Characteristic part of time series of the dynamics of the TC cell in response to Parkinsonian input ($g_{PD,max} = 0.3$ mS cm^{-2}, $g_{DBS} = g_{exc} = 0$). (A) the presynaptic GPi spike times; (B) the synaptic input s_{PD}; (C) the calcium inactivation gating variable h_T; (D) the membrane potential V of the TC cell for $g_A = 0$ (solid) and $g_A = 1.5$ mS cm^{-2} (dotted). The two traces are very similar except near $t = 2750$ ms when without the A-current there is a rebound, but not for the simulation with the A-current.
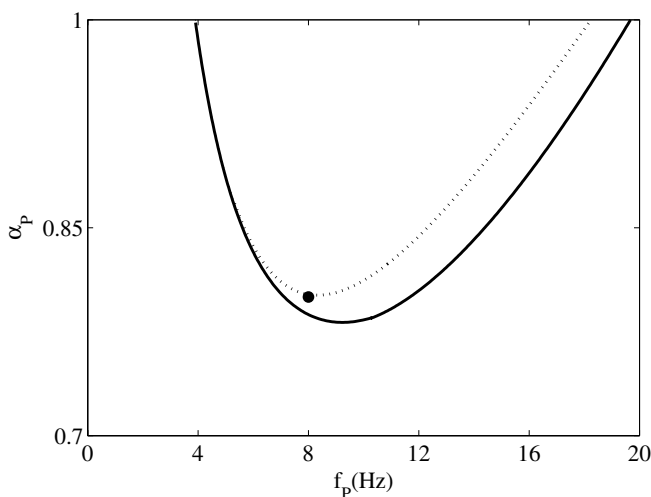

Figure 5. For the frequency range from 3 to 20 Hz the threshold levels for the generation of rebound action potentials (APs) and no rebound APs are plotted. The two curves indicating α_{c1} (dotted) and α_{c2} (solid) enclose a region of bistability. The dot represents the parameter values used in figure 6 ($g_{GPi,Th} = 0.1$ mS cm^{-2}).

The bi-stable behavior of the thalamic cell for this situation is presented in figure 6.

The instability boundaries of the spiking and non-spiking solutions consist of saddle-node and period-doubling bifurcations. These boundaries depend smoothly on other system parameters (Chow and Hale 1982, Kuznetsov 2004). We have investigated how these boundaries change for different values of $g_{GPi,Th}$. For other values of $g_{GPi,Th}$ the curves have a similar shape to those shown in figure 5. For f_P near 5 Hz, the boundaries exist for $g_{GPi,Th} \geqslant 0.075$ (or $g_{PD,max} \geqslant 0.15$); this accords with the result shown in figure 3. As $g_{GPi,Th}$ values increase, we noted that the minimum value of α_P (i.e. where the TC cell is most sensitive) is at lower values of f_P and the instability region narrows.

3.2. Stimulation of the TC cell: rebound suppression and relay reliability

The addition of stimulation-induced inhibitory and excitatory input alters the response of the TC cell. Depending on the parameters of the input, several qualitatively different scenarios exist. Examples of these different responses are shown in figure 7 in which the membrane potential of the TC cell and the excitatory input are presented. For the Parkinsonian signal derived from the GPi recording we set $g_{PD,max} = 0.4$ mS cm^{-2}. For the stimulation, we set the frequency $f_{DBS} = 135$ Hz, with a rate of activity increment $\beta = 1.2$ and the overwriting parameter ('stimulation amplitude') λ is set low (0.05), intermediate (0.1–0.2) or complete (1.0).

Without excitatory inputs ($g_{exc} = 0$) rebound responses still exist during low amplitude DBS (figure 7(A)). For intermediate values of g_{DBS}, rebounds are suppressed due to a little extra inhibition which keeps the membrane potential below a firing threshold (figure 7(B)). Even at low values of λ, many, but not all, rebounds are suppressed (figure 7(C)) in the presence of excitatory inputs. For intermediate strength of λ, rebounds completely disappear (figure 7(D)). As can be seen in the corresponding figures, most of the excitatory inputs were relayed. A stronger DBS signal, however, induces more inhibition causing relay failure (figure 7(E)). Relay failure also occurs if the strength of the excitatory inputs is too low (figure 7(F)). As soon as stimulation is stopped rebound activity re-appears. Note that only the scenarios shown in figures 7(B) and (D) seem desirable as both rebounds are suppressed and excitatory inputs are relayed sufficiently.

Next, we systematically varied the parameters λ and f_{DBS} to find regions with sufficient rebound suppression ($S > 0.9$) and relay reliability ($R > 0.9$) (see figure 8). For each frequency f_{DBS} we determine a value of the parameter λ corresponding to these thresholds resulting in S-curves and R-curves, respectively. In all panels, rebounds are suppressed *above* the S-curves (dashed) and sufficient relay occurs *below* the R-curves (bold).

Figures 8(A)–(D) show S-curves presenting the minimally required recruitment λ for a given stimulation frequency f_{DBS} in order to suppress transmission of the Parkinsonian drive
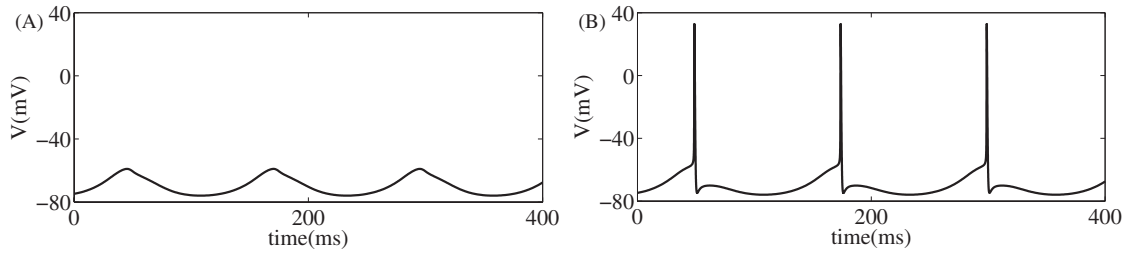
Figure 6. For $f_P = 8$ Hz, $\alpha_P = 0.8$ and $g_{\mathrm{GPi,Th}} = 0.1$ mS cm^{-2} the TC model neuron described by (1) has both stable non-spiking (A) and stable spiking (B) solutions. This region of bistability ranges from $\alpha_{c2} \approx 0.79 < \alpha_P < \alpha_{c1} \approx 0.81$.
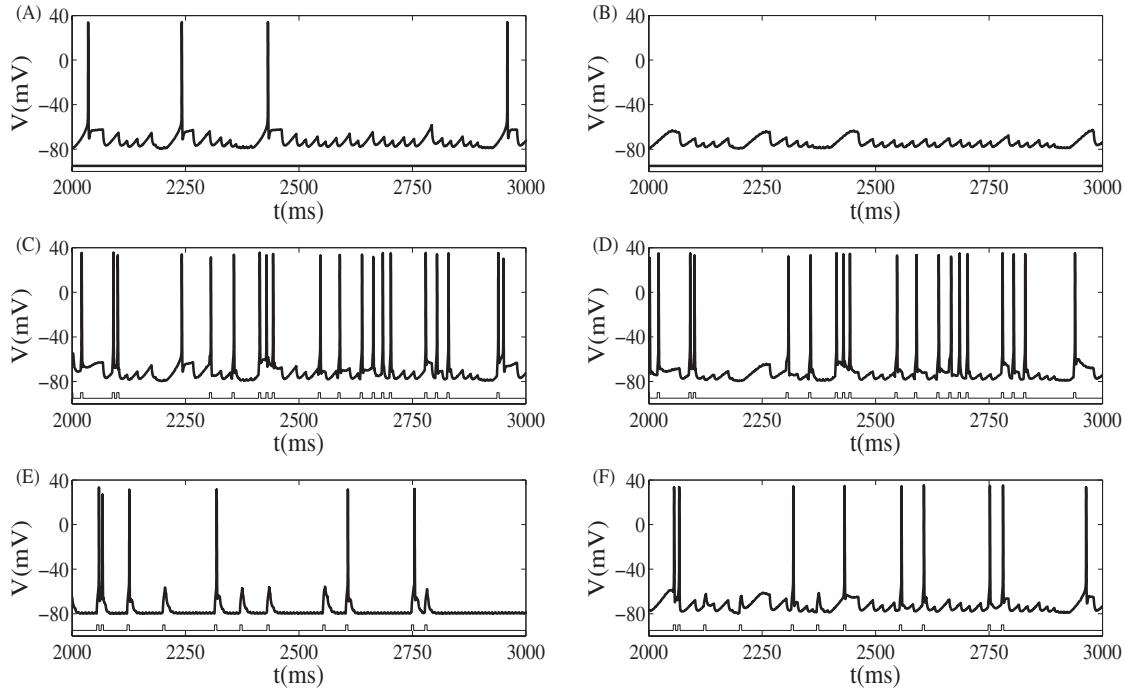

Figure 7. The behavior of the TC cell under Parkinsonian conditions for different stimulation settings. For the input (2) we fix $g_{\mathrm{PD,max}} = 0.4$ mS cm^{-2} and $\beta = 1.2$. The stimulation frequency is set at $f_{\mathrm{DBS}} = 135$ Hz. The upper traces represent the membrane voltage of the TC cell. For (C)–(F) the precise timing of the excitatory input (mean rate 16.5 Hz) is displayed beneath each voltage trace. (A) $\lambda = 0.05$ and $g_{\mathrm{exc}} = 0$: DBS too weak; (B) $\lambda = 0.2$ and $g_{\mathrm{exc}} = 0$: DBS sufficiently strong; (C) $\lambda = 0.05$ and $g_{\mathrm{exc}} = 0.15$: DBS too weak, still rebound responses; (D) $\lambda = 0.2$ and $g_{\mathrm{exc}} = 0.15$. Perfect relay and no rebounds; (E) $\lambda = 1.0$ and $g_{\mathrm{exc}} = 0.15$: relay failure due to too strong DBS; (F) $\lambda = 0.1$ and $g_{\mathrm{exc}} = 0.10$. Input too weak.

when no excitatory inputs are applied. For the *S*-curves (dashed) we could consider two cases: with and without excitatory input to be relayed. We find that these two curves hardly differ and that the one without relay is always slightly higher. Therefore, we present the case without relay only. Below we discuss the effect of the relay input on rebound suppression in more detail.

The *S*-curves show two asymptotes: for frequencies above 100 Hz an almost flat plateau occurs, while for lower stimulation frequencies the minimal recruitment λ increases. Stimulation below 40 Hz even fails to suppress rebound activity in most cases. The chance of an excitatory input occurring during high levels of inhibition, however, increases for higher f_{DBS}. When f_{DBS} is very high (>150 Hz), the minimum and maximum values of the synaptic variable s_{DBS} differ less and they are nearly constant. Therefore, the *R*-curve decreases for increasing f_{DBS}.

Most importantly, the combined *S*- and *R*-curves show that certain combinations of stimulation amplitude and

frequency, represented by λ and f_{DBS}, respectively, satisfy the condition for both sufficient relay (below *R*-curve) and rebound suppression (above *S*-curve). Within this amplitude–frequency window, the stimulation prevents transmission of the pathological oscillatory input, but does not impair the relay of sensorimotor input, provided this input is sufficiently strong. Generally speaking, this parameter window ranges for frequencies above 50 Hz and with λ between 0.15 and 0.3.

The size of this amplitude–frequency parameter window varies with slightly altered parameters. First, varying the strength of the excitatory input has a strong effect on the *R*-curve, but not the *S*-curve (figure 8(A)). This is as expected as it mainly influences the chance for successful relay. For low amplitudes of cortical input pulses the *R*-curve would overlap with or lie below the *S*-curve, e.g. R_1-curve for $g_{\mathrm{exc}} = 0.13$ mS cm^{-2}. In such cases, stimulation will not be able to both suppress rebounds and provide sufficient relay. Second, changing β from 1.0 to 2.0 confirms that the *R*-curve lowers with increasing β (figure 8(B)). This is
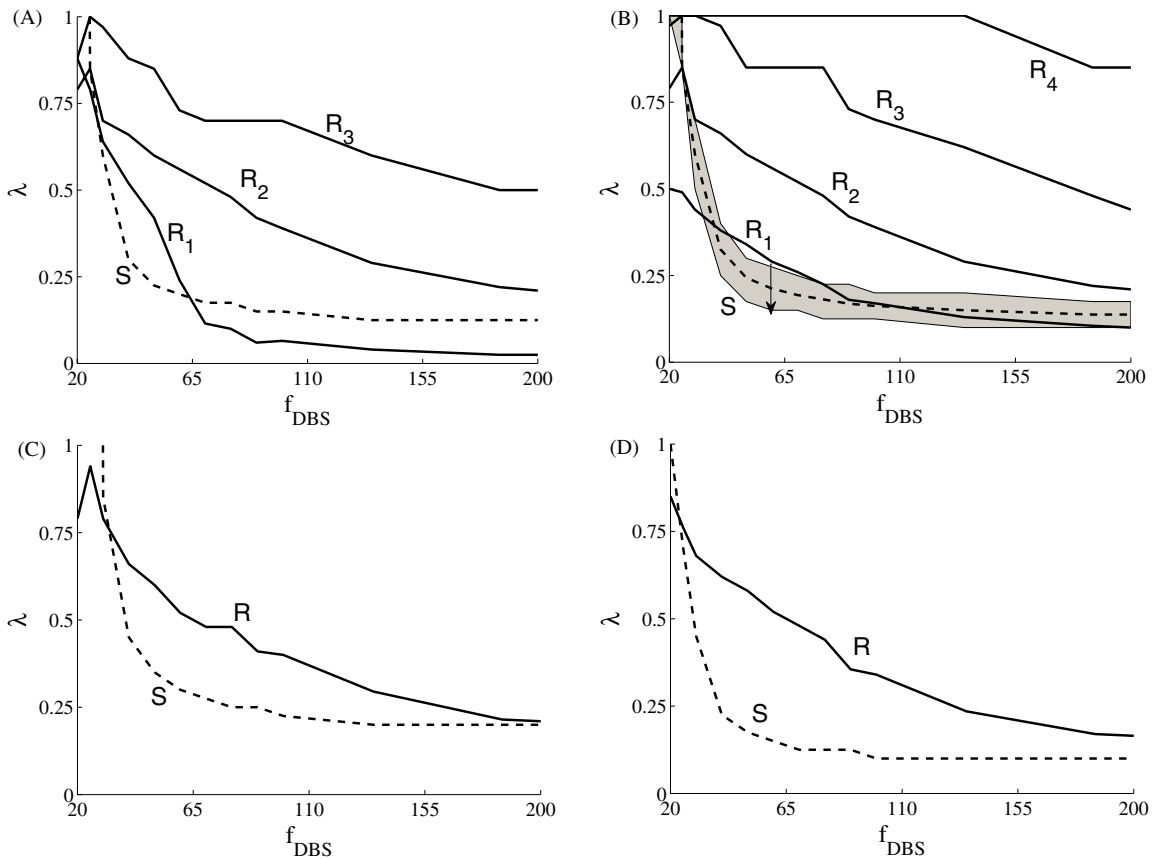
Figure 8. Sufficient suppression occurs above the *S*-curves (dashed), determined without relay ($g_{exc} = 0$), while sufficient relay is found below the *R*-curves (solid). Parameters are set to $g_{PD,max} = 0.4$ mS cm^{-2}, $\beta = 1.5$, $g_{exc} = 0.15$ mS cm^{-2}, $g_A = 0$ mS cm^{-2}, and $p_{Ca} = 0.1 \times 10^{-3}$ cm s^{-1} unless explicitly specified otherwise. (A) Different amplitudes for the excitatory input $g_{exc} = 0.13$ (R_1), 0.15 (R_2), 0.17 (R_3) mS cm^{-2}. (B) Different amplitudes for $\beta = 1.0$ (R_4), 1.2 (R_3), 1.5 (R_2), 2.0 (R_1). The arrow indicates the direction of increasing β. (C) Same as (A) with stronger T-current $p_{Ca} = 0.15 \times 10^{-3}$ cm s^{-1}. (D) Same as (A) with A-current $g_A = 1.5$ mS cm^{-2}.

expected: excitatory input is less easily relayed as the level of inhibition increases. Another trend, indicated by the arrow, is that increasing β also lowers the *S*-curves. This follows from the fact that stimulation with higher β induces more inhibition, which in turn makes it easier to suppress rebounds. As the shape of the four S-curves remains similar with varying β, we plot the mean of these curves together with the minimal and maximal value for each stimulation frequency indicated by a shaded area. Here the minimal and maximal λ differ by 0.075 only. Because the effect on the *R*-curve is much stronger than that on the *S*-curve, the window of suitable parameters is smaller for larger β. We also observed that with $\beta = 1.0$, in other words where there was no extra activity due to stimulation, there was only a minimum value of λ because sufficient relay still occurs for $\lambda = 1$ for most frequencies (R_4-curve). Third, a comparison of figures 8(A) and (C) reveals that a stronger T-current ($p_{Ca} = 0.15 \times 10^{-3}$ cm s^{-1} instead of 0.1×10^{-3}) makes it harder to suppress rebounds raising the *S*-curves. Another observation is that, during an excitatory input, the *T*-current provides some extra driving force that enables the relay to succeed; this makes the cell more responsive. This raises the *R*-curve. The combined effect is a smaller window. Fourth, the general effect of the A-current is that it slightly lowers the *R*- and *S*-curves by

impeding spiking a little. As a consequence, the amplitude–frequency window shifts to lower values of the amplitude only. Finally, we also tested the effect of different mean rates of the excitatory input $f_{exc} = 5$ in steps of 5–40 Hz, see figure 9, without DBS ($\lambda = 0$). We observe that for higher frequencies in the high-beta and low-gamma range many rebounds are suppressed by the excitatory input. This can be explained from the dynamics of the T-current, in particular the inactivation variable h_T. The excitatory input ($g_{exc} = 0.15$ mS cm^{-2}) ensures rapid inactivation of the T-type Ca^{2+}-channels, thereby preventing a rebound response. At the end of each GPi burst, therefore, the T-current is less de-inactivated in the presence of excitatory inputs. The higher the excitatory rate, the more often this occurs leading to increasing rebound suppression for higher rates.

Finally, we briefly mention that rebound activity is not suppressed by the application of low stimulation frequencies. First, stimulation applied without the oscillatory inhibitory and excitatory inputs ($\lambda \approx 1$) causes rebounds for low frequencies up to 21 Hz. However, in order to generate these rebounds, stimulation amplitudes needed to be higher than those used for the situations shown in figure 8 ($g_{DBS} > 0.4$ mS cm^{-2}). Second, low stimulation frequencies enhance the generation of rebound activity. In this case, even with weak Parkinsonian amplitudes, stimulation with a reasonably strong amplitude
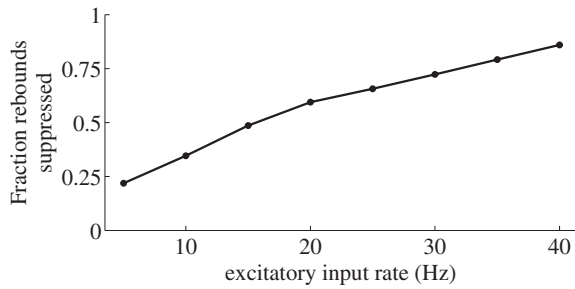
Figure 9. The fraction of rebounds suppressed due to the presence of the excitatory input increases with higher rates of the excitatory input.
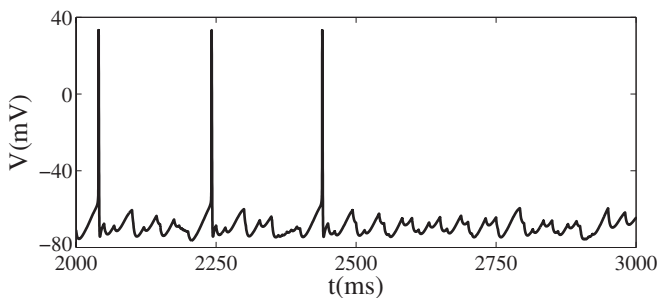

Figure 10. Time series of V during weak oscillatory Parkinsonian drive ($g_{PD,\max} = 0.25$ mS cm^{-2}), moderately strong stimulation ($\beta = 1.5$ and $\lambda = 0.5$) of low frequency ($f_{DBS} = 20$ Hz) and no excitatory input ($g_{exc} = 0$ mS cm^{-2}). Low frequency stimulation can enhance rebound responses.

($\lambda \approx 0.5$) partially overwrites the PD signal to the extent that this is no longer able to generate rebounds by itself. However, the combined PD and DBS signals still generate rebound activity (see figure 10). We have observed this enhancement for stimulation frequencies f_{DBS} up to 25 Hz. This contrasts with high frequencies, for which $\lambda \approx 0.2$ suppresses rebounds even where the then-weaker PD could generate rebounds (figure 8(A)).

4. Discussion

We investigated the modulation of TC functionality during DBS as a function of stimulation frequency and amplitude. We considered two effects of DBS on TC functionality, namely rebound suppression and relay suppression. We have shown that stimulation frequency influences the relay of low-frequency oscillations: low-stimulation frequencies enhance T-type rebound bursts, while high frequencies suppress them. The suppression of low-frequency oscillations requires a minimal stimulation amplitude, but too-high amplitudes block the relay of excitatory input. Taken together, this approach yields a parameter window that corresponds to therapeutic stimulation. Partial suppression of rebounds may also be achieved by applying excitatory input without stimulation.

It has been suggested that two principal modes of synchronized activity within the human subthalamo-pallidal-thalamo-cortical circuit are present: low frequency oscillations

(<30 Hz) facilitate slow idling rhythms in the motor areas of the cortex and high-frequency oscillations (>60 Hz) restore dynamic task-related cortical activity (Brown 2003). The numerical bifurcation analysis described here shows that the thalamic relay neuron responds to PD-related frequencies in the experimentally observed low-frequency range. This suggests that the TC cell could be involved in transmitting such slow rhythms to the motor cortex. The neuron becomes more responsive at lower frequencies when the amplitude of the input from GPi, $g_{GPi,Th}$, is increased. This indicates that frequency selectivity is an intrinsic property of the TC cell membrane. In particular, low frequency responses consist of rebound action potentials because the T-current is acting as a driving force in the generation of post-inhibitory action potentials. This extends an earlier observation in Cagnan *et al* (2009). Qualitative bifurcation theory (Chow and Hale 1982, Kuznetsov 2004) asserts the robustness of the neuron's behavior with respect to perturbations of other system parameters. Furthermore, frequency-dependent responses were previously discovered for thalamic cells in the investigations of Smith *et al* (2000, 2001) and Coombes *et al* (2001). Their approach explored the effect of an applied oscillating current within a reduced integrate-and-fire model for bursting with frequencies of 0.1–10 Hz. Note that a direct comparison between their setting and our synaptic pathway is not straightforward.

According to Brown (2003), a subdivision can be made in the lower frequency range and depending on the dominating direction of connectivity between GP and cortex. At frequencies below 10 Hz, the GPi leads and thus the net driving force for Parkinsonian rest tremor could be expected to occur through the GPi-thalamo-cortical pathway. Simulations in which the pathological oscillations are forwarded to the thalamus through GPi revealed that the TC neuron is most sensitive at a frequency band corresponding to the (rest) tremor frequencies observed in PD patients (see figure 5). Figures 5 and 6 show the result of bifurcation analysis revealing bi-stable behavior of the neuron, i.e. a non-spiking or silent mode and a rebound spiking mode. This bi-stability may be part of an explanation of the natural fluctuation in tremor intensity observed in PD patients (Timmermann *et al* 2002).

Model simulations reveal that rebound activity can be stopped by afferent sensory input directly to the thalamus, if the amplitude of the pathological low-frequency oscillation was not too high. This cortical (excitatory) input may involve sensory information (e.g. visual information for guidance of movements, or preparatory information for the execution of movements) being able to suppress PD tremor, as was observed by Amirnovin *et al* (2004). The presence of excitatory inputs makes it easier to suppress rebounds since (successful) relay disrupts calcium de-inactivation that generates a less de-inactivated state of the T-type channels. In turn, the driving force to generate a rebound spike is decreased. This may offer an indication why Parkinsonian rest tremor is usually absent during voluntary movement.

DBS may be effective through overwriting of PD activity and/or regularization of firing patterns (Rubin and Terman 2004, McIntyre *et al* 2004, Kuncel *et al* 2007). Rubin and

Terman (2004) assumed full overwriting such that increased GPi activity restores the relay functionality of TC cells. More recently, Cagnan demonstrated the link between stimulation amplitude and frequency with respect to the effectiveness of stimulation in a network model, and that full overwriting was unnecessary for restoring TC relay functionality (Cagnan *et al* 2009). Here, we considered the role of stimulation on TC function in more detail. In particular, we regard stimulation to be effective when the generation of rebound activity in response to oscillatory input at tremor frequencies is diminished and where the ability to relay cortical information is preserved. As shown in figure 8, successful relay occurs for amplitude–frequency combinations that remain below the *R*-curves. On the other hand, successful suppression of rebound activity requires that these combinations must be selected such that they remain above the *S*-curves. Therefore, the *R*- and *S*-curves represent the clinically effective window for stimulation. It follows that for frequencies below 40 Hz the stimulation amplitude must be high in comparison to stimulation frequencies above 70 Hz. This is in accordance with the observed inverse relationship between therapeutic frequency and amplitude (Benabid *et al* 1991, Limousin *et al* 1995, Gao *et al* 1999, Rizzone *et al* 2001). The window created by the *R*- and *S*-curves is reduced for lower frequencies.

We have shown that high-frequency DBS is effective even in the presence of a PD signal. This suggests that overwriting is not the main mechanism. Our explanation for the efficacy of high-frequency DBS is that a regularized input of moderate amplitude prevents rebound spike generation. Such regularization also underlies the effect of increasing rates of the relay input, which decreases the variance, (figure 9) and other recent computational studies (Cagnan *et al* 2009, Dorval *et al* 2010). When the DBS amplitude is too high, the relay functionality fails by overinhibition resulting in a loss of information. Relay functionality would also fail in the case of thalamotomy, i.e. ablating part of the thalamus. Thalamotomy and thalamic stimulation have been found to be equally effective, but thalamic stimulation results in a greater improvement in function (Schuurman *et al* 2000). This would suggest that during DBS thalamic relay output is preferable over no output after lesion. In our model, the efficacy of stimulation is tied to improvement of the relay functionality of the TC relay cells. Therefore, our model cannot explain the clinical improvement after lesion. To capture this effect, the entire basal ganglia–thalamocortical loop would need to be modeled to investigate whether thalamotomy leads to clinical improvement by disrupting the relay of low frequency oscillations around the loop by breaking the circuit at a key point. We have observed that the rebounds occur during silent periods after GPi bursts. This observation suggests a more efficient stimulation protocol if we intend to prevent the TC cell responding to a GPi burst. Then only temporary stimulation for suppressing rebounds might be needed. This might be more energy efficient and perhaps less distorting to other functional processes. However, we have used only a single recording of a single cell. This will probably be too unreliable to base a protocol upon. Therefore, we should investigate the GPi output of more cells and in local field potentials for population activity in a similar way as in Smirnov *et al* (2008).

Experimental observations show that (electrical) stimulation at frequencies below 60 Hz deteriorates PD symptoms (Rizzone *et al* 2001, Moro *et al* 2002, Timmermann *et al* 2004, Fogelson *et al* 2005, Eusebio *et al* 2008, Gradinaru *et al* 2009). Low frequency (<60 Hz) stimulation input in the model requires a higher stimulation amplitude to suppress rebound activity, the effect of which would disrupt the relay process. Moreover, for even lower stimulation frequencies (up to 20 Hz and within the beta band) the addition of stimulation may actually enhance the transmission of pathological BG oscillations, as shown in figure 10. Various system and input parameters have been varied to test the robustness of these qualitative findings. Although we have simulated only a single cell, this suggests that the response of a population of TC cells would be similar. It remains an open question how such a population responds if the TC cells are interconnected. Also here, the observation that excitatory inputs alone can partially suppress responses to GPi bursts could be tested in a TC population.

Our model is a gross simplification of the output and activity of the combined BG and cortico-thalamic network. We simulate only a single cell and we use a single recording for our pathological input. The input resulting from stimulation is idealized and the sensory input artificially generated. We also consider only a single pathological condition, i.e. tremor. Yet, the simulation's results are in good agreement with experimental data (Benabid *et al* 1991, Limousin *et al* 1995, Gao *et al* 1999). For some of our model input, we used experimental data in a method similar to that of Guo *et al* (2008). There is also scope for extending this method to measurements involving stimulation at several frequencies. As an intermediate step, the TC cell could be included in a network model that also includes STN, GPe and GPi neurons, with a view to aiding differentiation between STN and GPi stimulation similar to Pirini *et al* (2009). Assuming that low-frequency pathological oscillations in the range of 10–30 Hz are driven from the motor areas of the cortex (Brown 2003, Brown and Williams 2005), this work could also be extended by exploring the responses of such a network to such oscillations, particularly as they are most likely to be associated with anti-kinetic symptoms. It is an open question how to relate these symptoms with network activity in computational models. If this can be characterized with simple criteria, then one can explore the effect of stimulation on other pathological symptoms in computational models. In our model, the relation of rebounds to tremor is fairly straightforward and supported by experimental observations of tremor during recording. Other symptoms could very well result from interactions of multiple nuclei and their respective cells.

However, it must be kept in mind that pathophysiological changes in PD not only result from changes in firing patterns, but also from changes in firing rates, as well as changes in network connections. These lead in turn to, for example, the loss of functional segregation resulting in interference between competing motor circuits and a reduced ability to suppress unwanted movements (Molnar *et al* 2005, Moroney *et al* 2008). It could therefore be expected that stimulation is acting on the motor symptoms of PD by different mechanisms

(Temperli *et al* 2003). Supporting this hypothesis is the fact that tremor intensity is almost instantaneously reduced (within seconds) when the stimulation is applied, as is the case in our model. However, the alleviating of bradykinesia, rigidity and axial symptoms requires more time to take effect (minutes) (Johnson *et al* 2008). The same conclusion can be drawn from the fact that the effectiveness of DBS is different for the different symptoms over a 5 year period. Krack found that the worsening of akinesia, speech, postural stability, freezing of gait and cognitive function between the 1st and the 5th year were consistent with the natural history of the disease (Krack *et al* 2003).

In summary, this study primarily focuses on the effectiveness of DBS as a mechanism for reducing PD tremor. Our results show that the effectiveness of high-frequency DBS may result from selective suppression of the relay of oscillations from BG to TC circuitry at tremor frequencies. The relay of sensorimotor information is, however, not affected for mid-range to moderately high DBS amplitudes. Failure of the relay function is only observed at very high DBS amplitudes and would appear to be nearly independent of frequency. Our study further suggests that low-frequency DBS (< 20 Hz) may enhance the transmission of tremor signals from BG into thalamocortical circuits. This is in accordance with clinical results.

Acknowledgments

Appendix. Constants

Parameters for the gating variables in models (1) are based upon (Destexhe *et al* 1998, McCormick and Huguenard 1992, Huguenard and McCormick 1992, McIntyre *et al* 2004, Cagnan *et al* 2009) such that $X_\infty = \alpha_X/(\alpha_X + \beta_X)$ and $\tau_X = 1/(\alpha_X + \beta_X)$.

Sodium current $I_{Na} = g_{Na} m^3 h(V - E_{Na})$ with $\alpha_m = 0.32(V + 55)/(1 - \exp(-(V + 55)/4))$, $\beta_{Na} = -0.28(V + 28)/(1 - \exp((V + 28)/5))$, $\alpha_h = 0.12 \exp(-(V + 51)/18)$, $\beta_h = 4/(1 + \exp(-(V + 28)/5))$,

Potassium currents $I_{K,DR} = g_K n^4(V - E_K)$ and $I_{Ks} = g_{Ks} d(0.4 e_1 + 0.6 e_2)(V - E_K)$ and $I_A = g_A d(0.6 f_1^4 h_1 + 0.4 f_2^4 h_2)(V - E_K)$ with $\alpha_n = 0.032(V + 63.8)/(1 - \exp(-(V + 63.8)/5))$, $\beta_n = 0.5 \exp(-(V + 68.8)/40)$, $d_\infty = 1/(1 + \exp(-(V + 43)/17))^4$, $\tau_d = 2.5 + 0.253/(\exp((V - 81)/25.6) + \exp((V + 132)/18))$, $e_{1,2,\infty} = 1/(1 + \exp((V + 58)/10.6))$, $\tau_e 1 = 30.4 + 0.253/(\exp((V - 13.29)/200) + \exp(-(V +$

$130)/7.1))$, $\tau_{e2} = 2260$ if $V > -70$ and $\tau_{e2} = \tau_{e1}$ if $V \leqslant -70$, $f_{1,\infty} = 1/(1 + \exp(-(V + 60)/8.5))$, $f_{2,\infty} = 1/(1 + \exp(-(V - 36)/20))$, $\tau_{f,1,2} = 1/(\exp((V + 35.8)/19.7) + \exp(-(V + 79.7)/12.7))$, $h_{1,2,\infty} = 1/(1 + \exp((V + 78)/6.0))$, $\tau_{h,1} = 1/(\exp((V + 46)/5.0) + \exp(-(V + 238)/37.5))$ if $V < -63$ and $\tau_{h,1} = 19$ if $V \geqslant -63$, $\tau_{h,2} = \tau_{h,1}$ if $V < -73$ and $\tau_{h,2} = 60$ if $V \geqslant -73$,

Hyperpolarization activated cation current $I_h = g_K c^4(V - E_h)$ with $c_\infty = 1/(1 + \exp((V + 85)/5.5))$, $\tau_c = 1/(\exp(-15.45 - 0.086V) + \exp(-1.17 + 0.0701V))$,

T-type calcium current $I_T = m_T^2 h_T F(V, V, [Ca]_i, [Ca]_o)$ with $m_{T,\infty} = 1/(1 + \exp(-(V + 60)/6.2))$, $h_{T,\infty} = 1/(1 + \exp(-(V + 84)/4))$, $\tau_{m_T} = 0.204 + 0.333/(\exp(-(V + 135)/16.7) + \exp((V + 19.8)/18.2))$, $\tau_{h_T} = 9.33 + 0.333 \exp(-(V + 25)/10.5)$ if $V \geqslant -81$, $\tau_{h_T} = 0.333 \exp((V + 470)/66.6)$ if $V < -81$ and the Goldman–Hodgkin–Katz ion current equation for (1) is given by

$$F(V, [Ca]_i, [Ca]_o) = p_{Ca} \frac{Z^2 F^2 V}{RT}$$
$$\times \frac{[Ca]_i - [Ca]_o \exp(-ZFV/RT)}{1 - \exp(-ZFV/RT)}.$$

The membrane capacitance C is assumed to be unity and the reversal potentials are set to $E_{Na} = 45$, $E_K = -95$, $E_h = -43$ mV, the conductances to $g_{Na} = 30$, $g_K = 3$, $g_{Ks} = 0.7$, $g_h = 0.5$, $g_{Na,leak} = 0.0207$, $g_{K,leak} = 0.05$ mS cm^{-2}. For the calcium concentration: $k_{Ca} = 5.1821e - 5$, $[Ca]_{buf} = 0.00024$ mM, $[Ca]_o = 2$ mM, $\tau_{pump} = 5$ ms, $p_{Ca} = 10^{-4}$ cm s^{-1} the maximum T-type calcium channel permeability, Z is the charge of a calcium ion, F is Faraday's constant in J (V mol)$^{-1}$, R is the gas constant in J (K mol)$^{-1}$ and $T = 309.15$ K.

References

Amirnovin R, Williams Z, Cosgrove G and Eskandar E 2004 *J. Neurosci.* **24** 11302–6

Anderson M, Postupna N and Ruffo M 2003 *J. Neurophys.* **89** 1150–60

Benabid A 2003 *Curr. Opin. Neurobiol.* **13** 696–706

Benabid A, Chabardes S, Mitrofanis J and Pollak P 2009 *Lancet Neurol.* **8** 67–81

Benabid A, Pollak P, Gervason C, Hoffman D, Gao D, Hommel M, Perret J and Rougemont J 1991 *Lancet* **337** 403–6

Bour L, Contarino M, Foncke E, de Bie R, van den Munckhof P, Speelman J and Schuurman P 2010 *Acta Neurochir.* **152** 2069–77

Brown P 2003 *Mov. Disord.* **18** 357–63

Brown P, Oliviero A, Mazzone P, Insola A, Tonali P and Di Lazzaro V 2001 *J. Neurosci.* **21** 1033–8

Brown P and Williams D 2005 *Clin. Neurophys.* **116** 2510–9

Butson C and McIntyre C 2005 *Clin. Neurophys.* **116** 2490–500

Cagnan H, Meijer H, van Gils S, Krupa M, Heida T, Rudolph M, Wadman W and Martens H 2009 *Eur. J. Neurosci.* **30** 1306–17

Carlson J, Cleary D, Cetas J, Heinricher M and Burchiel K 2010 *J. Neurophysiol.* **103** 962–7

Chow S N and Hale J 1982 *Methods of Bifurcation Theory* (New York: Springer)

Coombes S, Owen M and Smith G 2001 *Phys. Rev.* E **64** 419141

Destexhe A, Neubig M, Ulrich D and Huguenard J 1998 *J. Neurosci.* **18** 3574–88

Destexhe A and Sejnowski T 2003 *Phys. Rev.* **83** 1401–53

Deuschl G, Raethjen J, Baron R, Lindemann M, Wilms H and Krack P 2000 *J. Neurol.* **247** 33–48

Dhooge A, Govaerts W and Kuznetsov Y 2003 *ACM Trans. Math. Softw.* **29** 141–64

Dolan K, Martens H, Schuurman P and Bour L 2009 *Med. Biol. Eng. Comput.* **47** 791–800

Dorval A, Kuncel A, Birdno M, Turner D and Grill W 2010 *J. Neurophysiol.* **104** 911–21

Dostrovsky J and Lozano A 2002 *Mov. Disord.* **17** 63–8

Eusebio A, Chen C, Lu C, Lee S, Tsai C, Limousin P, Hariz M and Brown P 2008 *Exp. Neurol.* **209** 125–30

Fogelson N, Kuhn A, Silberstein P, Limousin P, Hariz M, Trottenberg T, Kupsch A and Brown P 2005 *Neurosci. Lett.* **382** 5–9

Gao D, Benazzouz A, Piallat B, Bressand K, Ilinsky I, Kultas Ilinsky K and Benabid A 1999 *Neuroscience* **88** 201–12

Gradinaru V, Mogri M, Thompson K, Henderson J and Deisseroth K 2009 *Science* **324** 354–9

Guo Y, Rubin J, McIntyre C, Vitek J and Terman D 2008 *J. Neurophysiol.* **99** 1477–92

Hahn P and McIntyre C 2010 *J. Comput. Neurosci.* **28** 425–41

Hahn P, Russo G, Hashimoto T, Miocinovic S, Xu W, McIntyre C and Vitek J 2008 *Exp. Neurol.* **211** 243–51

Halliday D, Rosenberg J, Amjad A, Breeze P, Conway B and Farmer S 1995 *Prog. Biophys. Mol. Biol.* **64** 237–78

Hammond C, Bergman H and Brown P 2007 *Trends Neurosci.* **30** 357–64

Hashimoto T, Elder C, Okun M, Patrick S and Vitek J 2003 *J. Neurosci.* **23** 1916–23

Huguenard J and McCormick D 1992 *J. Neurophysiol.* **68** 1373–83

Jahnsen H and Llinàs R 1984 *J. Physiol.* **349** 205–26

Johnson M and McIntyre C 2008 *J. Neurophysiol.* **100** 2549–63

Johnson M, Miocinovic S, McIntyre C and Vitek J 2008 *Neurotherapeutics* **5** 294–308

Kim U, Sanchez-Vives M and McCormick D 1997 *Science* **278** 130–4

Krack P *et al* 2003 *N. Engl. J. Med.* **349** 1925–34

Kuncel A, Cooper S, Wolgamuth B and Grill W 2007 *IEEE Trans. Neural Syst. Rehabil. Eng.* **15** 190–7

Kuznetsov Y 2004 *Elements of Applied Bifurcation Theory* 3rd edn (Berlin: Springer)

Levy R, Hutchinson W, Lozano A and Dostrovsky J 2000 *J. Neurosci.* **20** 7766–75

Limousin P, Pollak P, Benazzouz A, Hoffmann D, Le Bas J, Broussolle E, Perret J E and Benabid A 1995 *Lancet* **345** 91–5

Lozano A, Dostrovsky J, Chen R and Ashby P 2002 *Lancet Neurol.* **1** 225–31

Magill P, Bolam J and Bevan M 2000 *J. Neurosci.* **20** 820–33

Magnin M, Morel A and Jeanmonod D 2000 *Neuroscience* **96** 549–64

McCormick D and Huguenard J 1992 *J. Neurophysiol.* **68** 1384–400

McIntyre C, Grill W, Sherman D and Thakor N 2004 *J. Neurophysiol.* **91** 1457–69

McIntyre C and Hahn P 2010 *Neurobiol. Dis.* **38** 329–37

Molineux M, Fernandez F, Mehaffey W and Turner R 2005 *J. Neurosci.* **25** 10863–73

Molnar G F, Pilliar A, Lozano A M and Dostrovsky J O 2005 *J. Neurophysiol.* **93** 3094–101

Montgomery E and Gale J 2008 *Neurosci. Biobehav. Rev.* **32** 388–407

Moro E, Esselink R, Xie J, Hommel M, Benabid A and Pollak P 2002 *Neurology* **59** 706–13

Moroney R, Heida C and Geelen J 2008 *J. Comput. Neurosci.* **25** 501–19

Nini A, Feingold A, Slovin H and Bergman H 1995 *J. Neurophysiol.* **74** 1800–5

Pape H, Budde T, Mager R and Kisvarday Z 1994 *J. Physiol.* **478** 403–22

Pirini M, Rocchi L, Sensi M and Chiari L 2009 *J. Comput. Neurosci.* **26** 91–107

Raz A, Vaadia E and Bergman H 2000 *J. Neurosci.* **20** 8559–71

Reese R, Steigerwald F, Pötter M, Herzog J, Deuschl G, Volkmann J, Pinsker M and Mehdorn H 2008 *Mov. Disord.* **23** 1945–7

Rizzone M, Lanotte M, Bergamasco B, Tavella A, Torre E, Faccani G, Melcarne A and Lopiano L 2001 *J. Neurol. Neurosurg. Psychiatry* **71** 215–9

Rubin J and Terman D 2004 *J. Comput. Neurosci.* **16** 211–35

Schuurman P R, Bosch D A, Bossuyt P M, Bonsel G J, van Someren E J, de Bie R M, Merkus M P and Speelman J D 2000 *N. Engl. J. Med.* **342** 461–8

Sherman S 2001 *Trends Neurosci.* **24** 122–6

Smirnov D, Barnikol U, Barnikol T, Bezruchko B, Hauptmann C, Bührle C, Maarouf M, Sturm V, Freund H J and Tass P 2008 *Europhys. Lett.* **83** 20003

Smith G, Cox C, Sherman S and Rinzel J 2000 *J. Neurophysiol.* **83** 588–610

Smith G, Cox C, Sherman S and Rinzel J 2001 *Thalamus Relat. Syst.* **1** 135–56

Smith Y, Bevan M, Shink E and Bolam J 1998 *Neuroscience* **86** 353–87

Tass P 2001 *Biol. Cybern.* **85** 343–54

Temperli P, Ghika J, Villemure J G, Burkhard P, Bogousslavsky J and Vingerhoets F 2003 *Neurology* **60** 78–81

Terman D, Rubin J, Yew A and Wilson C 2002 *J. Neurosci.* **22** 2963–76

Timmermann L, Gross J, Dirks M, Volkmann J, Freund H J and Schnitzler A 2002 *Brain* **126** 199–212

Timmermann L, Wojtecki L, Gross J, Lehrke R, Voges J, Maarouf M, Treuer H, Sturm V and Schnitzler A 2004 *Mov. Disord.* **19** 1328–33

Volkmann J, Herzog J, Kopper F and Geuschl G 2002 *Mov. Disord.* **17** S181–7

Volkmann J, Moro E and Pahwa R 2006 *Mov. Disord.* **21** S284–9